

Relativistic bands in the spectrum of created particles via dynamical Casimir effect

Andreson L. C. Rego¹, João Paulo da S. Alves², Danilo T. Alves² and C. Farina¹

1 - *Instituto de Física, Universidade Federal do Rio de Janeiro,
21945-970, Rio de Janeiro, RJ, Brazil*

2 - *Faculdade de Física, Universidade Federal do Pará, 66075-110, Belém, PA, Brazil*

(Dated: October 17, 2018)

We present a general analytical approach to investigate relativistic corrections in the dynamical Casimir effect (DCE). Particularly, we discuss the behavior of the additional frequency bands that appear in the spectral distribution of the created particles when the first relativistic corrections are taken into account. We do that in the context of circuit QED, by analyzing the setup used in the first measurement of the DCE, where a system with a time-dependent boundary condition simulates the mechanical motion of a single mirror in 1+1 dimensions. Our method is applicable to a large class of systems with oscillatory time-dependent parameters and can be generalized to higher dimensions and other fields.

PACS numbers: 31.30.jh, 03.70.+k, 42.50.Lc

I. INTRODUCTION

The theoretical prediction of the dynamical Casimir effect (DCE), essentially the conversion of vacuum fluctuations into real field excitations caused by moving mirrors, was made by Moore in 1970 [1]. This phenomenon was also investigated in other pioneering works by DeWitt [2] and Fulling and Davies [3, 4]. Soon it was realized that, in real experimental situations, the creation of photons via DCE using mechanical motions of material plates is negligible, since the highest velocity that a mirror can achieve under laboratory conditions is very small in comparison with the speed of light [1, 5, 6]. A way to circumvent this difficulty is to simulate a moving mirror by a physical mechanism which gives rise to a time-dependent boundary condition (BC) for the field at a fixed mirror, an ingenious idea, first proposed by Yablonovitch in 1989 [7]. Several experimental proposals for the detection of the DCE are based on the simulation of moving boundaries [8–12]. We should also mention an ingenious proposal involving real mechanical motion of boundaries suggested by Kim *et al* [13], in which the dynamical Casimir photons would trigger a superradiance process which would then be observed. One of these experimental proposals, based on a superconducting coplanar waveguide terminated by a SQUID (Superconducting Quantum Interference Device), led to the announcement by Wilson *et al* of the first observation of the DCE [14]. In this experiment, a time-dependent magnetic flux is applied to the SQUID, changing its effective inductance, resulting in a time-dependent BC, such that the coplanar waveguide becomes equivalent to a one-dimensional transmission line with variable length. This setup simulates a single moving mirror whose effective velocity can achieve approximately 10% of the speed of light [9].

The DCE for a one-dimensional model with a single mirror moving in vacuum, with oscillatory motion with frequency ω_0 , small amplitude and non-relativistic velocities, was investigated by Lambrecht *et al* [15]. These authors concluded that the spectral distribution of the created photons has a parabolic shape, with a maximum at $\omega_0/2$ and no particle created with frequencies higher than ω_0 [15]. In contrast, if the oscillatory motion has relativistic velocities, the same authors pointed out the presence of additional frequency bands in the spectrum of the created particles. These bands vanish for all frequencies ω equal to an integer multiple of ω_0 , so that the spectrum is decomposed into a succession of arches, each one limited by two successive multiples of ω_0 [5]. At that time, this model

was considered “not realistic as it would imply a mirror’s mechanical velocity appreciable compared to the speed of light” [5].

However, in the recent experiment made by Wilson *et al* [14], the effective velocities can achieve $\sim 10\%$ of the velocity of light. This fact motivated us to investigate relativistic effects in the particle creation via DCE, particularly, the emergence of an additional and experimentally detectable band in the spectral distribution. This additional band provides an extra signature for identifying dynamical Casimir photons. In the SQUID experiment, the DCE is modeled by a Robin BC at a fixed point but with a time-dependent Robin parameter. For this case, the relativistic corrections (additional bands) were theoretically predicted by Johansson *et al* [9]. In contrast with the model investigated in Ref. [5], the spectrum found in Ref. [9] does not vanish for frequencies ω equal to multiples of ω_0 , and each higher order band has a parabolic form going from 0 to an integer multiple of ω_0 . Robin BC in the DCE with moving plates were firstly investigated by Mintz *et al* [16]. A generalization to 3+1 dimensions was recently reported in the literature [17]. For Robin BC at fixed plates with time-dependent Robin parameter see Silva-Farina [18] and Fosco *et al* [19].

The shape of the additional bands investigated in Refs. [5] and [9] are different, and also were calculated via different approaches, namely: an analytical approach valid for a certain class of motions in $1 + 1$ dimensions [5] and a computer numerical method [9], respectively. However, there is absence in literature of a systematic analytical approach applicable to the DCE in a relativistic system with a general oscillatory time-dependent parameter and that can be generalized to higher dimensions. To fill this lack, in the present paper we develop a general perturbative analytical approach which enables the investigation of additional bands in the spectrum of created particles via DCE, computing, systematically, relativistic effects to any desired order. Although the main ideas of our approach are quite general, in the present work we shall focus on applications related to the problem of the DCE in a superconducting circuit [9, 14, 18].

The paper is organized as follows. In Sec. II, considering the SQUID experiment where the DCE is modeled by a Robin BC at a fixed point with a time-dependent Robin parameter, we develop a general formula which gives the complete perturbative solution for the spectral distribution of the created particles. In Sec. III, we use in the referred formula parameters related to the SQUID experiment, providing the experimentalists with some predictions.

Our final comments are in Sec. IV.

II. A GENERAL ANALYTICAL APPROACH FOR COMPUTING RELATIVISTIC CORRECTIONS

Let us start considering a superconducting coplanar waveguide with capacitance and inductance per unit length given, respectively, by C_0 and L_0 , and terminated through a SQUID (see Ref. [9]). Due to the presence of Josephson junctions in this system, according to [9] the electromagnetic field in this coplanar waveguide can be conveniently described by the phase field operator $\phi(t, x)$, defined by $\phi(t, x) = \int^t dt' E(t', x)$, where $E(t, x)$ is the electric field. It can be shown (see details in Ref. [9]) that the phase field obeys the massless Klein-Gordon equation $(v^{-2} \partial_t^2 - \partial_x^2)\phi(t, x) = 0$, where $v = 1/\sqrt{C_0 L_0}$ is the velocity of light in the waveguide (throughout this paper we shall assume $\hbar = v = 1$). Applying appropriately Kirchoff's laws to the superconducting circuit, the authors in [9] show that the BC satisfied by ϕ is the following

$$\phi(t, 0) - \gamma(t) (\partial_x \phi)(t, 0) \approx 0, \quad (1)$$

with $\gamma(t) = -\bar{\Phi}_0^2 [(2\pi)^2 E_J(t) L_0]^{-1} = -L_{\text{eff}}(t)$, where $\bar{\Phi}_0$ is the magnetic quantum flux, $E_J(t)$ is the effective Josephson energy (which depends on the magnetic flux), and $L_{\text{eff}}(t)$ is an effective length that modulates the change in time of the distance between the SQUID to an effective mirror at origin [9]. The previous equation corresponds to a Robin BC at a fixed point with a time-dependent Robin parameter. Considering the following general expression for the Josephson energy $E_J(t) = E_J^0 [1 + \epsilon f(t)]$, where $0 < \epsilon < 1$ and $|f(t)| < 1$, we can write the time-dependent Robin parameter as

$$\gamma(t) \approx \gamma_0 \left[1 + \sum_{k=1}^N \epsilon^k f_k(t) \right], \quad (2)$$

where $f_k(t) = [-f(t)]^k$, $\gamma_0 = -\bar{\Phi}_0^2 [(2\pi)^2 E_J^0 L_0]^{-1}$ and N denotes the order of expansion under investigation.

Now, we extend the Ford-Vilenkin perturbative approach [20] by expressing the field solution in the form

$$\phi(t, x) \approx \phi_0(t, x) + \sum_{j=1}^N \epsilon^j \phi_j(t, x), \quad (3)$$

where $\phi_0(t, x)$ is the unperturbed field and $\epsilon^j \phi_j(t, x)$ represents the correction of order j , with ϕ_0 and ϕ_j obeying the massless Klein-Gordon equation. The unperturbed field ϕ_0 obeys the usual static Robin BC at origin, $\phi_0(t, 0) = \gamma_0 \partial_x \phi_0(t, 0)$. As a consequence, the unperturbed field ϕ_0 is given, for $x > 0$,

$$\phi_0(t, x) = \frac{1}{2\pi} \int_{-\infty}^{\infty} dk \Phi_0(k, x) e^{-i\omega_k t},$$

where

$$\Phi_0(k, x) = \sqrt{\frac{4\pi}{\omega_k(1+k^2\gamma_0^2)}} g(k, x, \gamma_0) [a(k)\Theta(k) - a^\dagger(-k)\Theta(-k)], \quad (4)$$

with

$$g(k, x, \gamma_0) = \sin(kx) + k\gamma_0 \cos(kx). \quad (5)$$

In the previous equations, $\Theta(k)$ is the Heaviside function, $a^\dagger(k)$ and $a(k)$ are the creation and annihilation operators that satisfy the canonical commutation rule $[a(k), a^\dagger(k')] = \delta(k - k')$ and $\omega_k = |k|$. It can be shown that the fields ϕ_j obey the BC

$$\phi_j(t, 0) - \gamma_0 \partial_x \phi_j(t, 0) \approx \gamma_0 \sum_{k=1}^j f_k(t) \partial_x \phi_{j-k}(t, 0). \quad (6)$$

The time Fourier transform of the field $\phi_j(t, x)$, denoted by $\Phi_j(\omega, x)$, satisfies Helmholtz equation $(\omega^2 + \partial_x^2)\Phi_j(\omega, x) = 0$. Taking the Fourier transform of Eq. (6), we see that the field $\Phi_j(\omega, 0)$ satisfies to the following BC

$$[1 - \gamma_0 \partial_x] \Phi_j(\omega, 0) = \int_{-\infty}^{\infty} d\xi \left[\mathcal{O}_{\omega, \xi}^{(j)}(x) \Phi_0(\xi, x) \right]_{x=0}, \quad (7)$$

where

$$\begin{aligned} \mathcal{O}_{\omega, \xi}^{(j)}(x) &= \sum_{k=1}^j \int_{-\infty}^{\infty} \frac{d\xi_1}{2\pi} \frac{i\xi_1}{1 - i\xi_1\gamma_0} F_k(\omega - \xi_1) \mathcal{O}_{\xi_1, \xi}^{(j-k)}(x), \\ \mathcal{O}_{\xi_1, \xi}^{(0)}(x) &= (i\xi_1)^{-1} (1 - i\xi_1\gamma_0) \delta(\xi_1 - \xi) \partial_x, \end{aligned} \quad (8)$$

represent recurrence formulas for the operators $\mathcal{O}_{\omega, \xi}^{(j)}(x)$ that act on the spatial part of the unperturbed field $\Phi_0(\omega, x)$, and F is the Fourier transform of f . As causality requires, the solution $\Phi_j(\omega, x)$ of the Helmholtz equation must lead to a solution $\phi_j(t, x)$ that travels from the mirror to infinity. The time Fourier transform of $\phi(t, x)$ can be written as

$$\Phi(\omega, x) \approx \Phi_0(\omega, x) + \sum_{j=1}^N \epsilon^j \Phi_j(\omega, x). \quad (9)$$

Considering that $\gamma(t \rightarrow -\infty) = \gamma_0$, the in field Φ_0^{in} can be written as Φ_0 in Eq. (4), with a and a^\dagger relabeled as a_{in} and a_{in}^\dagger . Analogously, considering that $\gamma(t \rightarrow \infty) = \gamma_0$, the out field Φ_0^{out} can be written as Φ_0 in Eq. (4), with a relabeled as a^{out} . The in and out fields are then related by

$$\Phi_0^{\text{out}}(\omega, x) = \Phi_0^{\text{in}}(\omega, x) - \frac{1}{\gamma_0} [G^{\text{ret}}(\omega; x, 0) - G^{\text{adv}}(\omega; x, 0)] [1 - \gamma_0 \partial_x] \left[\sum_{j=1}^N \epsilon^j \Phi_j(\omega, x) \right]_{x=0}, \quad (10)$$

where the advanced and retarded Green functions are given by

$$G_{\text{adv}}^{\text{ret}}(\omega; x, 0) = \gamma_0 [1 \mp i\omega\gamma_0]^{-1} e^{\pm i\omega x}. \quad (11)$$

Using Eq.(4) and substituting the Green's function in equation linking Φ_0^{out} and Φ_0^{in} , we get the correspondent Bogoliubov transformation

$$a_{\text{out}}(\omega) = a_{\text{in}}(\omega) + \int_{-\infty}^{\infty} d\xi \sqrt{\frac{1}{|\xi| (1 + \xi^2 \gamma_0^2)}} \sum_{j=1}^N \epsilon^j \mathcal{G}^{(j)}(\omega, \xi) [a_{\text{in}}(\xi) \Theta(\xi) - a_{\text{in}}^\dagger(-\xi) \Theta(-\xi)], \quad (12)$$

where

$$\mathcal{G}^{(j)}(\omega, \xi) = 2i \sqrt{\frac{\omega}{1 + \omega^2 \gamma_0^2}} \left\{ \mathcal{O}_{\omega, \xi}^{(j)}(x) g(\xi, x, \gamma_0) \right\}_{x=0}. \quad (13)$$

For the case $N = 1$ we find the correspondent formula found in Ref. [18]. The linear dependence of a_{out} in terms of a_{in}^\dagger clearly indicates a non-vanishing particle creation distribution in the out state.

Since we are interested in computing the conversion caused by $\gamma(t)$ of vacuum fluctuations into real field excitations, we consider the vacuum ($|0_{\text{in}}\rangle$) as the in state of the system. From the Bogoliubov transformations (12), we obtain a very general formula (in 1+1 dimensions) for the number of created particles between ω and $\omega + d\omega$ per unit frequency, namely,

$$\mathcal{N}(\omega) = \langle 0_{\text{in}} | a_{\text{out}}^\dagger(\omega) a_{\text{out}}(\omega) | 0_{\text{in}} \rangle \approx \sum_{j,k=1}^{N'} \int_{-\infty}^{\infty} d\xi \frac{\epsilon^{j+k} \Theta(-\xi)}{|\xi| (1 + \xi^2 \gamma_0^2)} \mathcal{G}^{(j)*}(\omega, \xi) \mathcal{G}^{(k)}(\omega, \xi). \quad (14)$$

where $\sum_{j,k=1}^{N'}$ means that the indices j and k are chosen so that $j+k \leq N+1$. In other words, Eq. (14) gives the perturbative solution for the spectral distribution $\mathcal{N}(\omega)$ up to order $N+1$ in ϵ , and for an arbitrary time-dependence of the Robin parameter given according to Eq. (2).

III. APPLICATION TO THE SQUID EXPERIMENT

Hereafter we consider, for practical purposes, a particular application of the formula (14) for a typical oscillatory time variation of the Robin parameter given by $f(t) = \cos(\omega_0 t) e^{-|t|/\tau}$, with $\omega_0 \tau \gg 1$ (monochromatic limit) [9, 18], where ω_0 is the characteristic frequency and τ is the effective time interval in which the oscillations occur. In this context, Eq. (14) requires the solution of integrals having the general form $\int_{-\infty}^{\infty} d\omega A(\omega) B(\omega, \omega_0 \tau, \omega_i)$, where, as $\omega_0 \tau \rightarrow \infty$, the functions $B(\omega, \omega_0 \tau, \omega_i)$'s exhibit sharpened peaks at $\omega = \omega_i$'s, so that, in solving these integrals, we can apply

$$\lim_{\omega_0 \tau \rightarrow \infty} \int_{-\infty}^{\infty} d\omega A(\omega) B(\omega, \omega_0 \tau, \omega_i) = \left[\sum_i A(\omega_i) \right] \int_{-\infty}^{\infty} d\omega B(\omega, \omega_0 \tau, \omega_i). \quad (15)$$

Hereafter we also consider the following parameters related to the SQUID experiment: $\omega_0 = 2\pi \times 10.30$ GHz, $\epsilon = 0.25$, $v = 1.2 \times 10^8$ m/s and $\gamma_0 = 0.44 \times 10^{-3}$ m [9, 14]. For $N = 1$, Eq. (14) gives the non-relativistic analytical result $\mathcal{N}(\omega) \approx \epsilon^2 \mathcal{N}_2(\omega)$, with the analytical formula for $\mathcal{N}_2(\omega)$ being the same as that found in Ref. [18], and whose parabolic behavior is showed in Fig. 1, where we can observe that the spectrum is null for $\omega > \omega_0$. For $N = 2$, we get a negligible correction (proportional to ϵ^3) to the parabolic first band in the spectrum ($\mathcal{N}_3 \approx 0$).

Now, let us include the relativistic corrections. Considering $N = 3$, we get several integrals to be solved and, after several cumbersome calculations, we get a long final analytical formula for $\mathcal{N}(\omega)$, which can be represented by $\mathcal{N}(\omega) \approx \epsilon^2 \mathcal{N}_2(\omega) + \epsilon^4 \mathcal{N}_4(\omega)$, where $\epsilon^4 \mathcal{N}_4(\omega)$ describes the relativistic corrections in the spectral density. Since the analytical formula for $\mathcal{N}_4(\omega)$ is too long to be written here, we just exhibit its graphical behavior in Fig. 2 (solid line). We observe that $\mathcal{N}_4(\omega)$ is null for $\omega > 2\omega_0$. Notice that \mathcal{N}_4 contributes either to correct the non-relativistic band $\epsilon^2 \mathcal{N}_2$ in the region $0 < \omega < \omega_0$, as to compose the additional part in the region $\omega_0 < \omega < 2\omega_0$ of the spectrum. A subtle difference between our result and the one found in Ref. [9] is that the additional band $\epsilon^4 \mathcal{N}_4$ does not have exactly the parabolic form going from 0 to $2\omega_0$, as considered in [9]. After adding $\epsilon^2 \mathcal{N}_2$ with $\epsilon^4 \mathcal{N}_4$, we get the shape shown in Fig. 3 (dashed line), which is in good agreement with the one obtained via numerical methods in Ref. [9].

Let us now provide the experimentalists with some predictions. From our calculations, we obtain that, in the non-relativistic approximation ($\epsilon^2 \mathcal{N}_2$), the rate of photon creation

is $5.8 \times 10^6/\text{sec}$, and the maximum frequency is $\omega = \omega_0$. Taking into account the first relativistic correction ($\epsilon^2 \mathcal{N}_2 + \epsilon^4 \mathcal{N}_4$), the range of frequencies of the created particles is extended up to $2\omega_0$, the rate of photon creation is enhanced to $6.2 \times 10^6/\text{sec}$ (6% greater in relation to the non-relativistic result), and the rate of created particles with frequencies $\omega_0 < \omega < 2\omega_0$ (relativistic band) is $1.8 \times 10^5/\text{sec}$. These photons with frequencies in the interval $\omega_0 < \omega < 2\omega_0$ may, in principle, be observed, providing this way an extra signatures for the identification of the dynamical Casimir effect.

Finally, as an additional check for our analytical formulas, we investigate the toy model in which we prescribe the time behavior of the parameter $\gamma(t)$ such that it is exactly given by $\gamma(t) = \gamma_0[1 + \epsilon f_1(t)]$. It is possible to show that this model approximately describes a moving mirror imposing a Dirichlet boundary condition to the field. Now, the function $\mathcal{N}_4(\omega)$ is relabeled as $\mathcal{N}_4^{(1)}(\omega)$, and, after adding $\epsilon^2 \mathcal{N}_2$ with $\epsilon^4 \mathcal{N}_4^{(1)}$, we get the shape shown in Fig. 4 (dashed line). This shape is in agreement with the prediction (see Ref. [5]) of additional bands vanishing for all frequencies ω equal to an integer multiple of ω_0 , with the spectrum decomposed into a succession of arches, each one limited by two successive multiples of ω_0 , and with two points of maximum: one of them slightly shifted to the left in relation to $\omega_0/2$, and the other one shifted to the right in relation to $3\omega_0/2$.

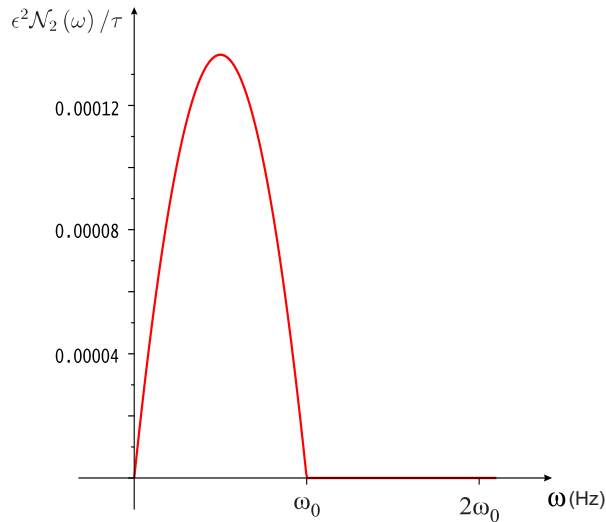


FIG. 1. (color online) First (non-relativistic) parabolic band $\epsilon^2 \mathcal{N}_2(\omega)/\tau$.

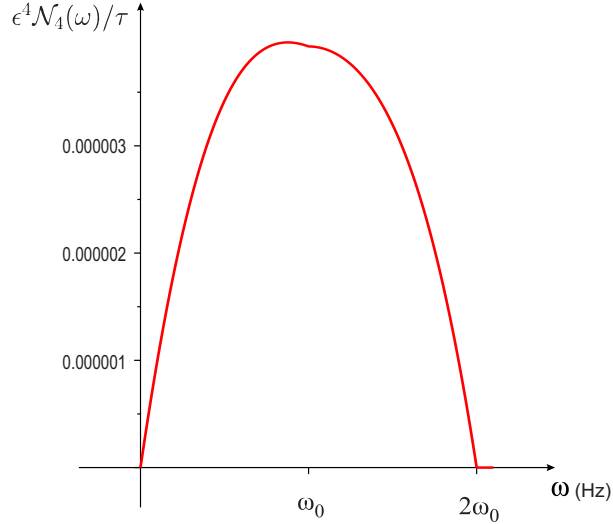


FIG. 2. (color online) First relativistic correction $\epsilon^4 \mathcal{N}_4(\omega)/\tau$.

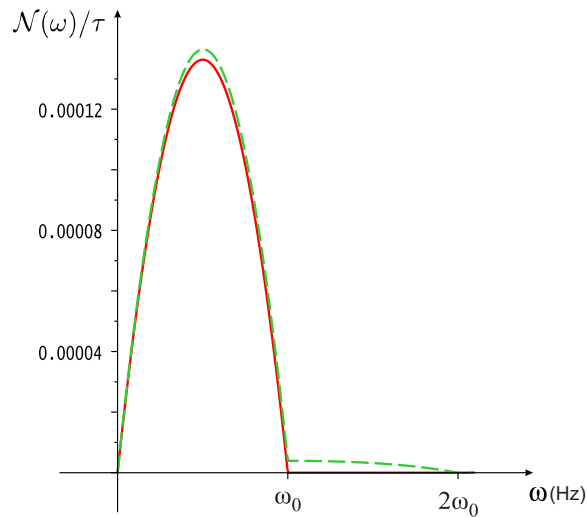


FIG. 3. (color online) The solid line is the first (non-relativistic) parabolic band $\epsilon^2 \mathcal{N}_2(\omega)/\tau$. The dashed line is $\mathcal{N}(\omega) = [\epsilon^2 \mathcal{N}_2(\omega) + \epsilon^4 \mathcal{N}_4(\omega)] / \tau$.

IV. FINAL REMARKS

In this work we presented an analytical approach to the DCE which includes systematically relativistic effects to any desired order. We applied our method to the model which describes theoretically the setup used in the SQUID experiment [9]. We made estimatives of the first relativistic effects, providing the experimentalists with theoretical predictions to be tested. Particularly, we estimated the intensity of the first relativistic band (relativistic

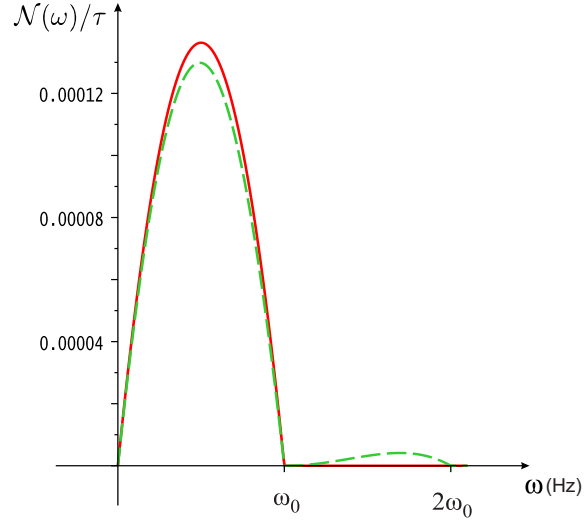


FIG. 4. (color online) The solid line is the first (non-relativistic) parabolic band $\epsilon^2 \mathcal{N}_2(\omega)/\tau$. The dashed line is $\mathcal{N}(\omega) = [\epsilon^2 \mathcal{N}_2(\omega) + \epsilon^4 \mathcal{N}_4(\omega)] / \tau$.

effect) relative to the first one (non-relativistic result). It is very important to take into account these corrections because they may provide an extra signature for identifying the dynamical Casimir photons. The observation of an additional frequency band would be a remarkable experimental achievement.

Finally, we remark that the generalization of the Ford-Vilenkin approach [20], shown in the present work, to investigate the appearance of additional bands in the spectral density, considering the theoretical model underlying the SQUID experiment, requires not only the generalization given by the Eq. (3), but also includes (2). Only taking into account both generalizations, one can reproduce the bands shown in Figs. 2 (solid line) and 3 (dashed line), in agreement with the numerical results found in Ref. [9]. Though our calculations were made in 1+1 dimensions, because we were interested in discussing the SQUID experiment, our approach can be generalized to other systems, higher dimensions, different fields (electromagnetic fields, massive fields...) and boundary conditions.

V. ACKNOWLEDGMENTS

We thank J.D.L. Silva, A.N. Braga, P.A. Maia Neto and C.M. Wilson for valuable discussions. This work was partially supported by CNPq, CAPES and FAPERJ.

-
- [1] G.T. Moore, J Math. Phys. **11**, 2679 (1970).
 - [2] B.S. DeWitt, Phys. Rep. **19**, 295 (1975).
 - [3] S.A. Fulling and P.C.W. Davies, Proc. R. Soc. London **A 348**, 393 (1976).
 - [4] P.C.W. Davies and S.A. Fulling, Proc. R. Soc. London **A 354**, 59 (1977).
 - [5] A. Lambrecht *et al*, Eur. Phys. J. D **3**, 95 (1998).
 - [6] V.V. Dodonov and A.B. Klimov, Phys. Rev. A, **53**, 2664 (1996).
 - [7] E. Yablonovitch, Phys. Rev. Lett. **62**, 1742 (1989);
 - [8] C. Braggio *et al*, Europhys. Lett **70**, 754 (2005); A. Agnesi *et al*, J. Phys. A **41**, 164024 (2008);
A. Agnesi *et al*, J. Phys: Conf. Series **161**, 012028 (2009).
 - [9] J.R. Johansson, G. Johansson, C.M. Wilson and F. Nori, Phys. Rev. Lett. **103**, 147003 (2009);
J.R. Johansson, G. Johansson, C.M. Wilson and F. Nori, Phys. Rev. A **82**, 052509 (2010).
 - [10] F.X. Dezael and A. Lambrecht, Eur. Phys. Lett. **89**, 14001 (2010).
 - [11] T. Kawakubo and K. Yamamoto, Phys. Rev. A, **83**, 013819 (2011).
 - [12] D. Faccio and I. Carusotto, Eur. Phys. Lett **96**, 24006 (2011).
 - [13] W.J. Kim, J.H. Brownell and R. Onofrio , Phys. Rev. Lett. **96**, 200402 (2006).
 - [14] C.M. Wilson *et al*, Nature (London) **479**, 376 (2011).
 - [15] A. Lambrecht, M.T. Jaekel and S. Reynaud, Phys. Rev. Lett. **77**, 615 (1996).
 - [16] B. Mintz *et al*, J. Phys. A **39**, 6559 (2006); B. Mintz *et al*, J. Phys. A **39**, 11325 (2006).
 - [17] Andreson L. C. Rego, B.W. Mintz, C. Farina and D.T. Alves, Phys. Rev. D **87**, 045024 (2013).
 - [18] H. O. Silva and C. Farina, Phys. Rev. D **84**, 045003 (2011).
 - [19] C.D. Fosco, F.C. Lombardo and F.D. Mazzitelli, Phys. Rev. D **87**, 105008 (2013).
 - [20] L.H. Ford and A. Vilenkin, Phys. Rev. D **25**, 2569 (1982).